FIXITY FOR SPUDCANS BEARING ON SAND UNDER CLAY

J.S. Templeton, III*
SAGE USA, Inc.
* *corresponding author: j*ackt@sage-usa.com

ABSTRACT
For site specific assessment of jack-up rigs, applicable standards and practices provide for establishment of certain spudcan fixity parameters. Among the parameters are the maximum moment capacity, the maximum horizontal capacity and various stiffness factors. These parameters are established by use of site-specific soils data, spud can geometry, and preload values. ISO 19905-1[1] provides procedures for determination of fixity parameters for all-clay soil profiles and for all-sand profiles. Importantly, however, the standard does not provide any guidance for the case of deep penetration through clay to bear on underlying sand – a situation which often occurs in practice and one of considerable importance.

This paper presents results from numerical analysis for the important case of penetration through clay onto deep sand as well as recommendations for the determination of both stiffness and capacity factors.

KEY WORDS: Jack-up Rigs, Site-Specific Assessment, Spudcan Foundations, Fixity.

INTRODUCTION

Among the parameters to be used for site specific assessment of jack-up rigs are certain spudcan fixity parameters: the maximum moment capacity factor, the maximum horizontal capacity factor, and three initial stiffness factors. Values for these parameters can be established by use of formulae involving site-specific soils data, spud can geometry, and preload values.

Procedures are provided by ISO 19905-1[1] for determination of fixity parameters for all-clay soil profiles and for all-sand profiles. Importantly, however, the standard does not provide any guidance for the case of deep penetration through clay to bear on underlying sand – a situation which often occurs in practice and one of considerable importance. A study was undertaken to address this situation. The objective of this study was to determine fixity parameters (initial stiffness depth factors, K_{d1}, K_{d2} and Kd3, as well as capacity factors, Cm and Ch) for spudcans bearing on sand deep under a clay layer. Numerical analyses were performed to establish fixity estimates for this important case, and recommendations were formed for the determination of factors for the needed stiffness and capacity factors.

WORK PERFORMED

Analyses with the Abaqus program were used to provide numerical solutions for the in-place loading of spudcans bearing on sand deep under a clay layer. Abaqus [2] is a large, nonlinear, general purpose, commercial finite element analysis program with substantial soil mechanics capabilities. It has a long history of successful use in offshore geotechnical analysis (See Templeton [3]).

Traditionally, finite element analysis has been accomplished using what is now called a Lagrangian approach. In this approach, nodes and element boundaries are tied to material, and a fixed body of material is contained in each element. The mesh deforms with the material, and the amount of material deformation that can be achieved is ultimately limited by errors resulting from element deformation. With an Eulerian approach the nodes and element boundaries are fixed in space and material flows across element boundaries as material deformations occur without any element deformation. In this way arbitrarily large material deformations can be achieved without element performance problems. In Abaqus Coupled Eulerian-Lagrangian (CEL) analysis, Lagrangian meshing for bodies with limited deformation can be combined with Eulerian meshing for bodies with large deformations, and contacting surfaces of the two kinds of bodies can interact. In addition, large deformation theory (including large strain formulations for both stress and strain as well as proper treatment of large rotations and the effects of essential geometry change) is used throughout all steps of CEL analyses in both Lagrangian and

Eulerian bodies. Both Lagrangian and CEL analyses were used in this study.

The stiffness case analyses reported here were performed as small strain Lagrangian analyses with the spudcan represented by a "wished-in-place" disk. This was done because the initial stiffness is inherently a small strain parameter and also for consistency with the basis in Bell [4] for the stiffness depth factors already provided in ISO 19905-1 [1]. Figure 1 shows the model and approach used for the stiffness case analyses. The following are notable aspects of the analyses:

- Small strain analysis with linear elastic materials
- Uniform clay layer over uniform sand
- Both sand and clay taken as practically incompressible.
- Spudcan as rigid circular disk of zero thickness at the clay/sand interface
- No-slip conditions between disk and sand as well as between disk and clay
- Various ratios of clay shear modulus to sand shear modulus (G_{clay}/ G_{sand}) were analyzed
- Various ratios of clay embedment depth to spudcan diameter (D/ B) were analyzed
- Analyses were performed both for full backfill and for no backfill
- Separate analyses were performed for vertical, horizontal and moment loading
- Stiffness depth factors (K_{d1}, K_{d2}, K_{d3}.as defined in ISO 19905 [1]) were determined from analysis results.

The capacity case analyses were large deformation Abaqus CEL analyses. CEL and other large deformation finite element approaches have been used for other analyses of various spudcan foundation performance problems (see, for example, Templeton [5], Vazquez et al. [6] and Wang et al. [7]). Note that the Wang et al.[7] study dealt with spudcan foundations in clay underlain by sand, while the present study dealt with spudcan bearing on sand beneath clay. These two studies could be considered complementary.

Figure 2 shows the model and approach used for the stiffness case analyses. In these cases, the spudcan was modeled as a Lagrangian body, and the soil was modeled as an Eulerian body. The soil and spudcan were able to connect via a contact surface. In each case analysis the spudcan was loaded in three stages:

1. penetration from the mudline downward through the clay under the action of an increasing vertical load until bearing on the sand was achieved at a predetermined preload.
2. reduction of the vertical load to one half of the preload value.
3. Application of either a (rocking) rotation or a horizontal displacement with the vertical load maintained at one half of the preload value.

The following are additional details of the capacity case analyses:

- The contact surface was made rough on contact, but free to separate without adhesion.
- The spudcan geometry was based on a Letourneau 116-C with the forged tip removed and the corners rounded. These simplifications improved the contact surface performance
- The spudcan diameter was 46 ft (14 m), and the depth of the clay-sand interface was set at 60 ft (18.2 m) or 1.3 times the spudcan diameter.
- The spudcan was made rigid
- The clay was modeled as an elastic-plastic solid with a Tresca yield condition and normally consolidated shear strength (having negligible value at the mudline and increasing linearly with depth)
- The sand was modeled as an elastic-plastic solid with a Mohr-Coulomb yield condition with negligible cohesion and uniform angle of internal friction
- Ranges of values were investigated for preload, clay unit weight and clay strength gradient, as well as for sand friction angle and unit weight.

RESULTS

The results from the finite elements analyses are summarized in Tables A and B. Table A provides the results for stiffness depth factors, K_{d1} (vertical), K_{d2} (horizontal) and K_{d3} (rotational) – all determined consistently with ISO 19905-1 [1]. Results are presented for 24 stiffness analysis cases, including results

for all three directions and for the effects of backfill, depth of clay and Poisson's ratio – all for four different ratios of clay to sand shear modulus. Since the stiffness case analyses were performed as small strain linear analyses, the ratios of moment to rotation or force to displacement results were constant for each case. These ratios were used directly as stiffnesses to determine the stiffness depth factors in Table A.

Table B provides the results for the capacity factors, C_m (for rocking moment capacity) and C_h (for horizontal force capacity) – both determined consistently with ISO 19905-1 [1]. Results are presented for 18 capacity analysis cases, including results for both directions, each under nine combinations of variations in preload, clay strength gradient, and clay unit weight, as well as in sand friction angle and unit weight. Progressive reaction and displacement results were recorded from all 18 of the capacity case analyses. The maximum moment and horizontal force values needed for determination of the C_m and C_h values given in Table B were found by inspection of force vs. displacement and moment vs. rotation plots from these data.

Figure 3 presents the plot of moment vs. rotation from the base case rotational analysis. A relative peak moment is achieved at about 2.5 degrees of rotation, and the moment does not exceed this value until the rotation exceeds about 5 or 6 degrees, beyond which the moment increases to considerably greater values at much larger rotations. Such larger rotations would not customarily be tolerated, and such larger moments may be considered large rotation effects not of interest. Results of all rotational capacity cases showed achievement of either peak or plateau moment at similarly small rotations, followed by similar large rotation effects. In all cases, the small rotation peak or plateau moment value was used in the determination of C_h.

Figure 4 presents the plot of horizontal force vs. displacement from the base case horizontal analysis. A relative peak force is achieved at a displacement of about 3% of the spudcan diameter, and the force does not exceed this value until the displacement exceeds about 5% of diameter, beyond which the force increases to considerably greater values at much larger displacements. Such larger displacements would not customarily be tolerated, and such larger reaction forces may be considered large displacement effects not of interest. Results of all horizontal capacity cases showed achievement of either peak or plateau force at similarly small rotations, followed by similar large rotation effects. In all cases, the small displacement peak or plateau horizontal force value was used in the determination of C_h.

INTERPRETATION AND RECOMMENDED FORMULAE

Figures 5 through 8 present the stiffness depth ratio results from Table A in graphical form. Each of these figures provides two or three plots of stiffness depth ratio results vs. the ratio of clay to sand shear moduli, in comparison to proposed formulae. Figure 5 shows vertical, horizontal and rotational cases. Figure 6 shows the effect of backfill. Figure 7 shows the effect of the clay/sand interface depth. Figure 8 shows the effect of Poisson's ratio. Following are the proposed formulae, which were developed from the principle of superposition for linear systems.

$$K_{d1,s\backslash c} = 1 + G_{clay}/G_{sand}\,(K_{d1} - 1), \text{ vertical} \quad (1)$$

$$K_{d2,s\backslash c} = 1 + G_{clay}/G_{sand}\,(K_{d2} - 1), \text{ horizontal} \quad (2)$$

$$K_{d3,s\backslash c} = 1 + G_{clay}/G_{sand}\,(K_{d3} - 1), \text{ rotational} \quad (3)$$

where K_{d1}, K_{d2} and K_{d3} are the stiffness depth factors tabulated in ISO 19905-1 Table A.9.3-6; $K_{d1,s\backslash c}$, $K_{d2,s\backslash c}$ and $K_{d3,s\backslash c}$ are the stiffness depth factors for sand under clay and G_{clay}/G_{sand} is the ratio of clay shear modulus to sand shear modulus. The FEA results agree sufficiently well to support the use of the proposed formulae.

Figures 9 and 10 present the capacity factor results from Table B in graphical form. Each of these figures provides a plot of FEA results vs. a proposed formula. Figure 9 shows the results for the moment capacity factor, C_m, and Figure 9 shows the results for the horizontal capacity factor, C_h. Following are the proposed formulae:

$$C_{m,s\backslash c} = C_{m,sa} + f_m(C_{m,cl,deep} - C_{m,cl,shallow}), \text{ moment} \quad (4)$$

with $$f_m = 3.621 + 5.412\ \gamma'_{clay}/\gamma_w + 31.792\ (dS_u/dz)/\gamma_w - 1.162\ \tan(\varphi) - 1.979\ V_{LO}/Ap_a \quad (5)$$

$$C_{h,sa\backslash c} = C_{h,sa} + f_h(C_{h,cl,deep} - C_{h,cl,shallow}), \text{ horizontal} \quad (6)$$

with $$f_h = 0.629 + 0.908\ \gamma'_{clay}/\gamma_w + 5.427\ (dS_u/dz)/\gamma_w + 0.224\ \tan(\varphi) - 0.358\ V_{LO}/Ap_a \quad (7)$$

where:

$C_{m,sa}$, $C_{h,sa}$, $C_{m,cl,deep}$, $C_{m,cl,shallow}$, $C_{h,cl,deep}$ and $C_{h,cl,shallow}$ are per ISO 19905-1 for all-sand and all-clay soils
γ'_{clay}/γ_w is the submerged unit weight of clay, normalized by the standard unit weight of water
$(dS_u/dz)/\gamma_w$ is the strength gradient of clay, normalized by the standard unit weight of water
$\tan(\varphi)$ is the tangent of the sand friction angle
V_{LO}/Ap_a is the preload bearing pressure, normalized by standard atmospheric pressure.

The common form of the formulae for $C_{m,s\backslash c}$ and $C_{h,s\backslash c}$ was assumed intuitively and for convenience. The coefficients in the formulae for f_m and f_h were derived by linear regression on the FEA results. In both cases the regression slopes were essentially equal to unity, and the R^2 values exceeded 0.999. The FEA results correlate sufficiently well to support the use of the proposed formulae.

In the case of spudcan bearing on sand under a deep clay layer, from the work of this study, that fixity be evaluated by use of stiffness depth factors based on formulae (1) and (2) and capacity factors based on formulae (4) through (7).

ACKNOWLEDGEMENTS

The work reported here was sponsored by the International Association of Drilling Contractors (IADC) Jack-up Operators Committee. The IADC is gratefully acknowledged for its sponsorship of the work and for permission to publish this paper. On behalf of IADC, David R. Lewis of Lewis Engineering Group, James Brekke of Brekke Offshore Consulting, and Xiying Zhang of ABS provided considerable technical guidance during the course of the work.

The CEL modeling techniques used in this study drew significantly upon techniques used in prior studies with significant contributions to modeling and analysis techniques by SAGE engineers Frances Biegler and Matthew Barrett.

David Edwards of DNV is gratefully acknowledged for check and correction of the recommended formulae for initial stiffness.

REFERENCES

[1] ISO 19905-1, 3rd ed. Site-specific assessment of mobile offshore units – Part 1: Jack-ups. International Organization for Standardization, 2023.

[2] SIMULIA. Abaqus User's Guide, Dassault Systemes, Providence, RI, 2016

[3] Templeton JS, III, Finite element analysis in offshore geotechnics – a thirty-year retrospective, SIMULIA Customer Conference, 2012.

[4] Bell RW, The Analysis of Offshore Foundations subjected to combined loading, MSc. Thesis, University of Oxford, 1991

[5] Templeton JS, III, Jack-up spud can foundation fixity for various clay strength profiles, Proceedings of the 24th Offshore Symposium, Houston, TX, 2019.

[6] Vazquez JH, Grasso BD, Gamino MA, Templeton JS, III (2017) Using CEL to account for seabed deformation effects for jack-ups going of location, Proc.22nd Offshore Symposium, Houston, TX, 2017.

[7] Wang Y, Cassidy MJ, Bienen B, Numerical investigation of spudcan foundations in clay overlying sand under combined loading, J. Geotechnical and Geoenvironmental Engineering, 146(11), 04020117, 2020.

FIXITY FOR SPUDCANS BEARING ON SAND UNDER CLAY INITIAL STIFFNESS

Approach:

- small strain elastic FEA
- uniform sand under uniform clay layer
- circular disk at sand top
- various G_{clay}/G_{sand}
- various D/B
- full backfill or none
- V, H or M loading
- Results for K_{d1}, K_{d2}, K_{d3}

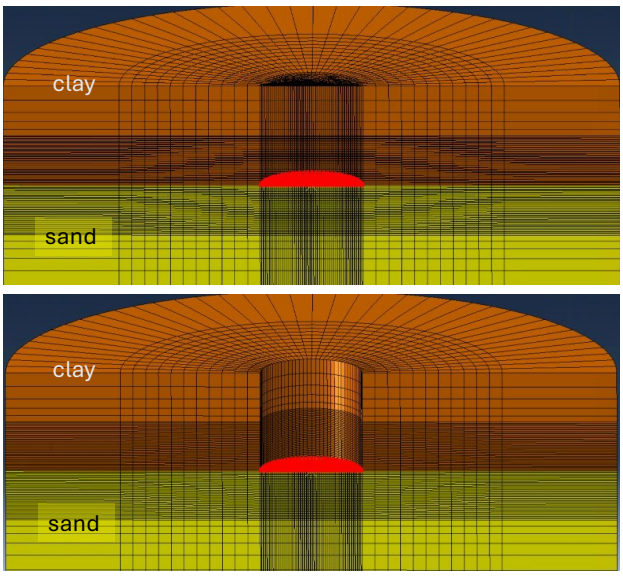

FIGURE 1: Model for stiffness analyses

FIXITY FOR SPUDCANS BEARING ON SAND UNDER CLAY CAPACITY

Approach:

- large deformation (CEL), nonlinear FEA
- uniform sand below D/B = 1.3 under normally consolidated clay layer
- spudcan penetrated under preload to bear on sand
- variations of preload, clay strength gradient, clay unit weight, sand ϕ and unit weight
- H or M loading applied after preload and de-ballast to preload/2
- Results for C_h, C_m

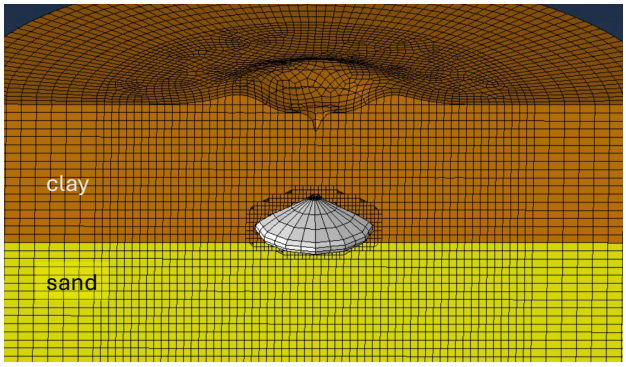

FIGURE 2: Model for capacity analyses

CASE	D/B	Backfill	Poisson's	Load		K_{dn}, FEA result for given G_{clay}/G_{sand}			
			ratio, nu	direction	n	Gcl/Gsa	Gcl/Gsa	Gcl/Gsa	Gcl/Gsa
						= 0.2	= 0.4	= 0.6	= 0.8
Base vertical	1.0	full	0.45	vertical	1	1.123	1.202	1.273	1.338
Base horizontal	1.0	full	0.45	horizontal	2	1.207	1.323	1.428	1.522
Base rotational	1.0	full	0.45	rotational	3	1.248	1.438	1.617	1.791
Backfill effect	1.0	none	0.45	rotational	3	1.139	1.212	1.284	1.355
Depth effect	0.5	full	0.45	rotational	3	1.208	1.346	1.477	1.606
Poisson effect	1.0	full	0.2	rotational	3	1.256	1.478	1.694	1.898

TABLE A: Summary of stiffness cases and results

CASE	V_{LO}	V_{LO}	S_u gradient	S_u gradient	clay ɣ'	clay ɣ'	sand ɣ'	sand ɣ'	sand ϕ	C_m	C_h
	kips	MN	pcf	kN/m^3	pcf	kN/m^3	pcf	kN/m^3	degrees	FEA result	FEA result
Base	12000	53.4	8.33	1.31	38	6.0	73	11.5	35	0.132	0.229
High V_{LO}	14400	64.1	8.33	1.31	38	6.0	73	11.5	35	0.114	0.199
Low V_{LO}	10000	44.5	8.33	1.31	38	6.0	73	11.5	35	0.153	0.256
High S_u gradient	12000	53.4	10.00	1.57	38	6.0	73	11.5	35	0.143	0.238
Low S_u gradient	12000	53.4	6.00	0.942	38	6.0	73	11.5	35	0.112	0.196
High clay ɣ'	12000	53.4	8.33	1.31	48	7.5	73	11.5	35	0.140	0.241
Low clay ɣ'	12000	53.4	8.33	1.31	28	4.4	73	11.5	35	0.113	0.205
High sand ϕ	12000	53.4	8.33	1.31	38	6.0	82	12.9	40	0.128	0.231
Low sand ϕ	12000	53.4	8.33	1.31	38	6.0	64	10.1	30	0.133	0.224

TABLE B: Summary of capacity cases and results

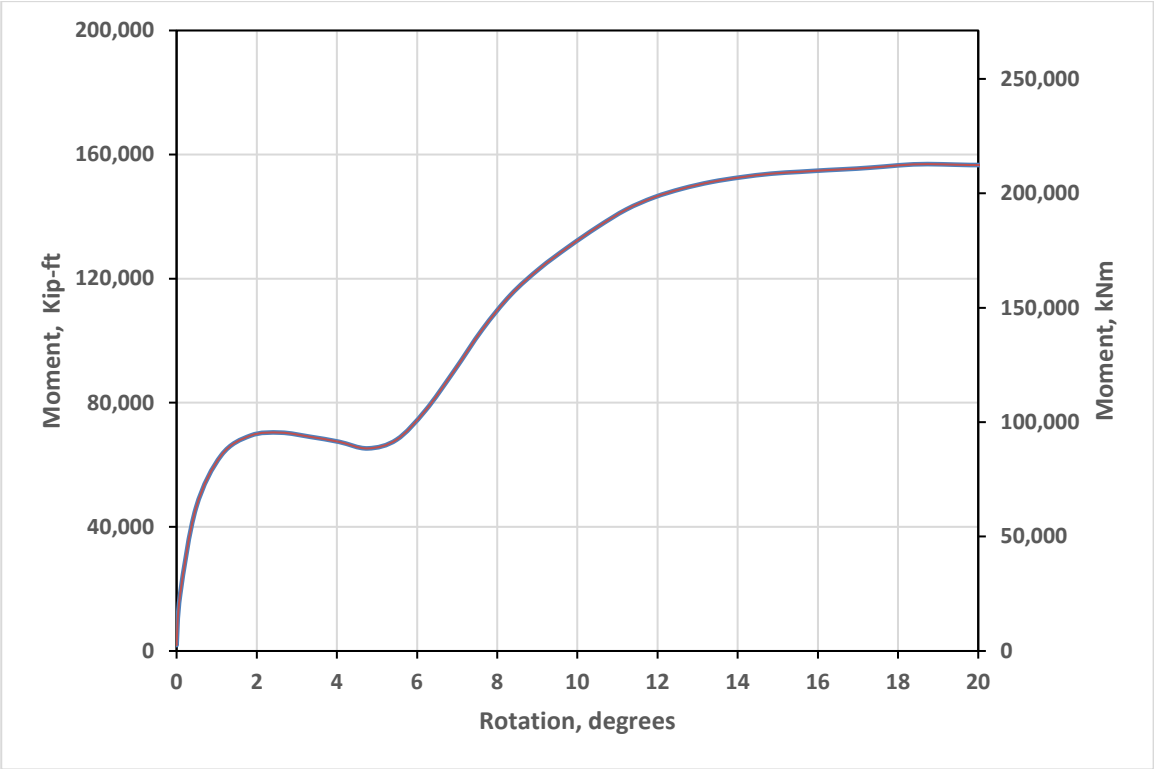

FIGURE 3: Plot of spudcan moment vs. rotation for Base Case

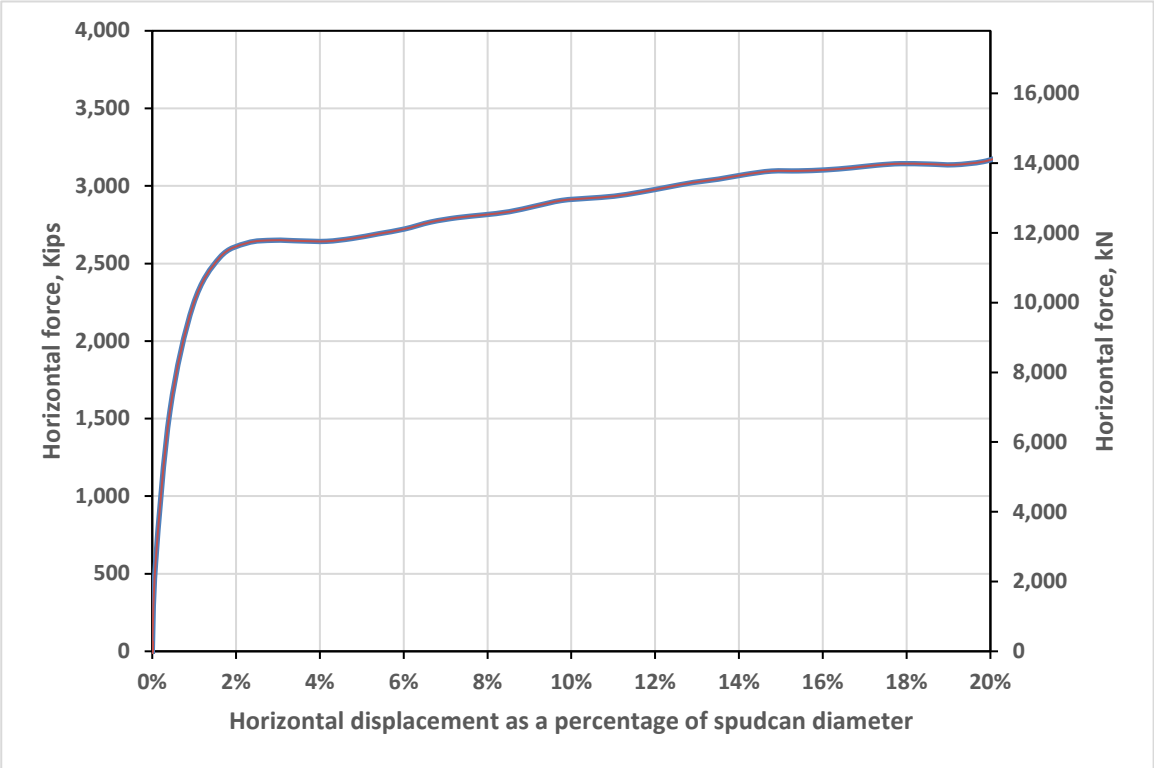

FIGURE 4: Plot of horizontal force vs. horizontal displacement for Base Case

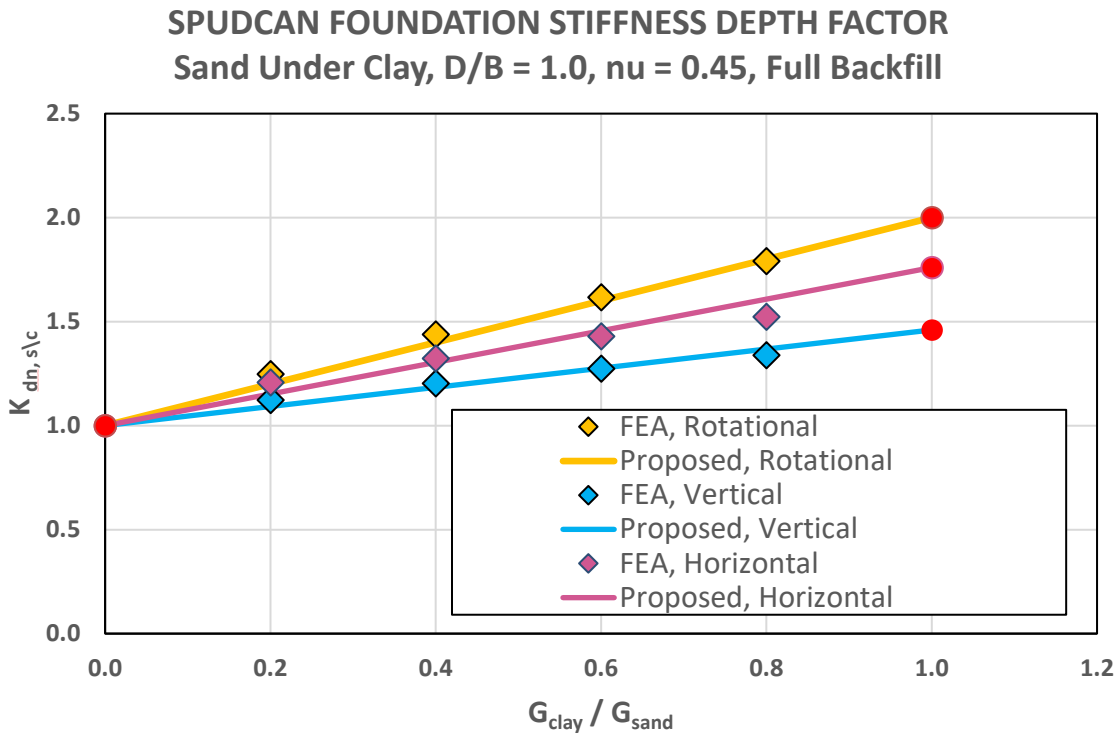

FIGURE 5: Spudcan foundation stiffness depth factor, sand under clay, D/B = 1.0, nu = 0.45, full backfill, compared to proposed formulation

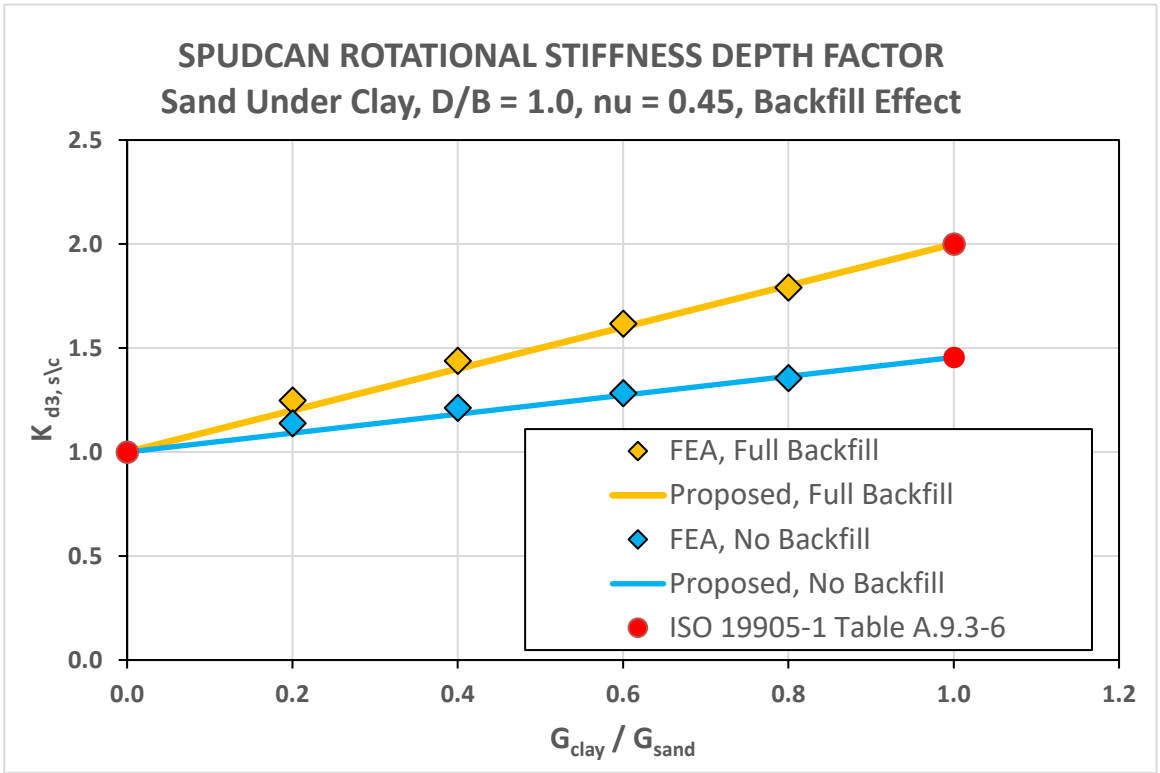

FIGURE 6: Spudcan foundation stiffness depth factor, sand under clay, D/B = 1.0, nu = 0.45, backfill effect, compared to proposed formulation

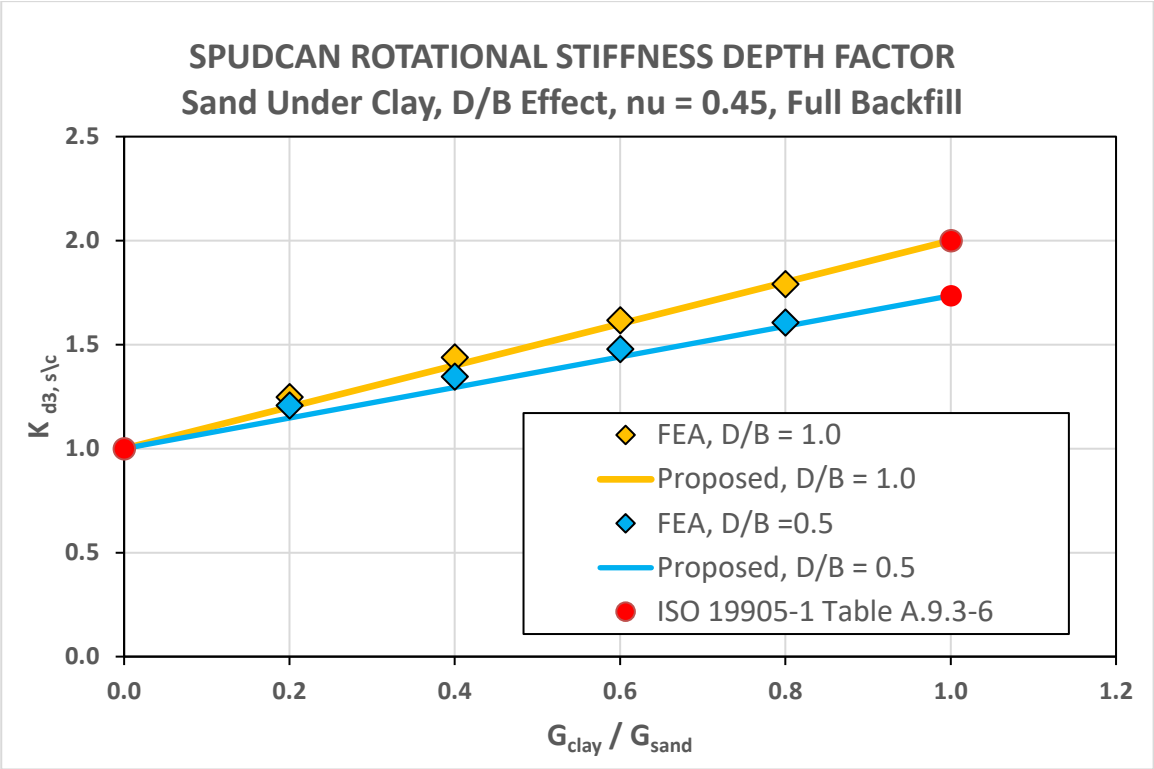

FIGURE 7: Spudcan foundation stiffness depth factor, sand under clay, D/B effect, nu = 0.45, full backfill, compared to proposed formulation

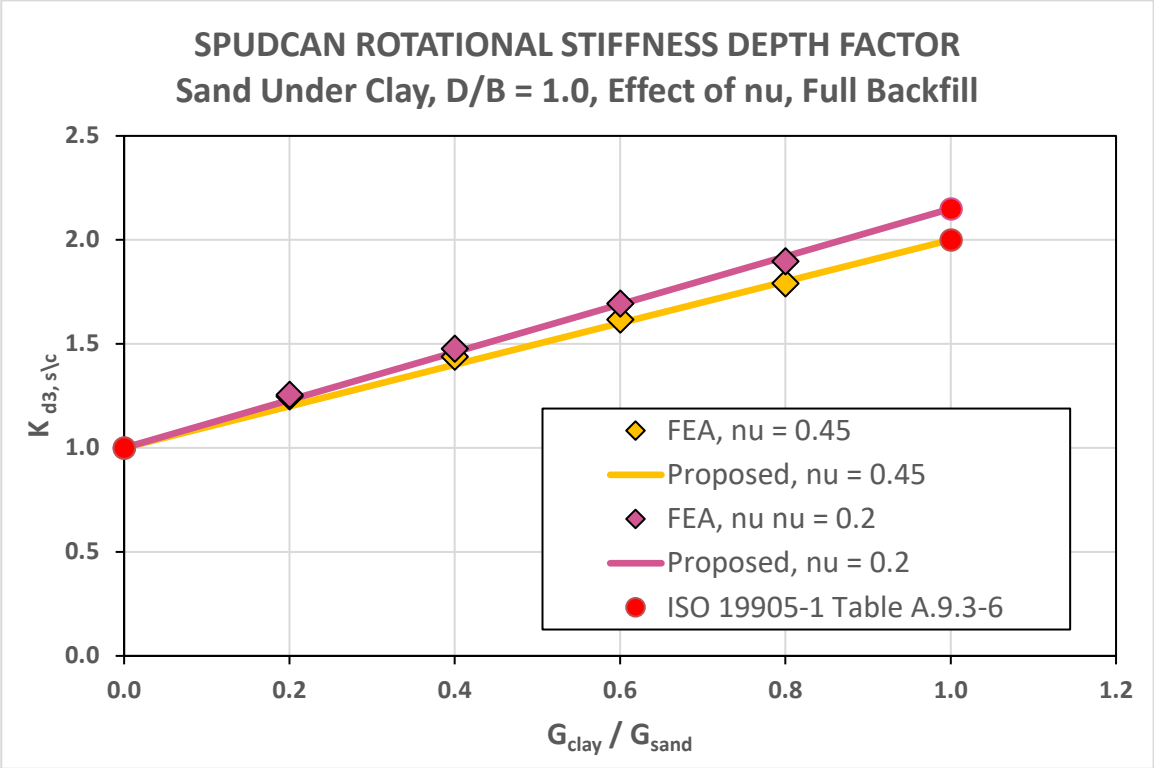

FIGURE 8: Spudcan foundation stiffness depth factor, sand under clay, D/B = 1.0, effect of nu, full backfill, compared to proposed formulation

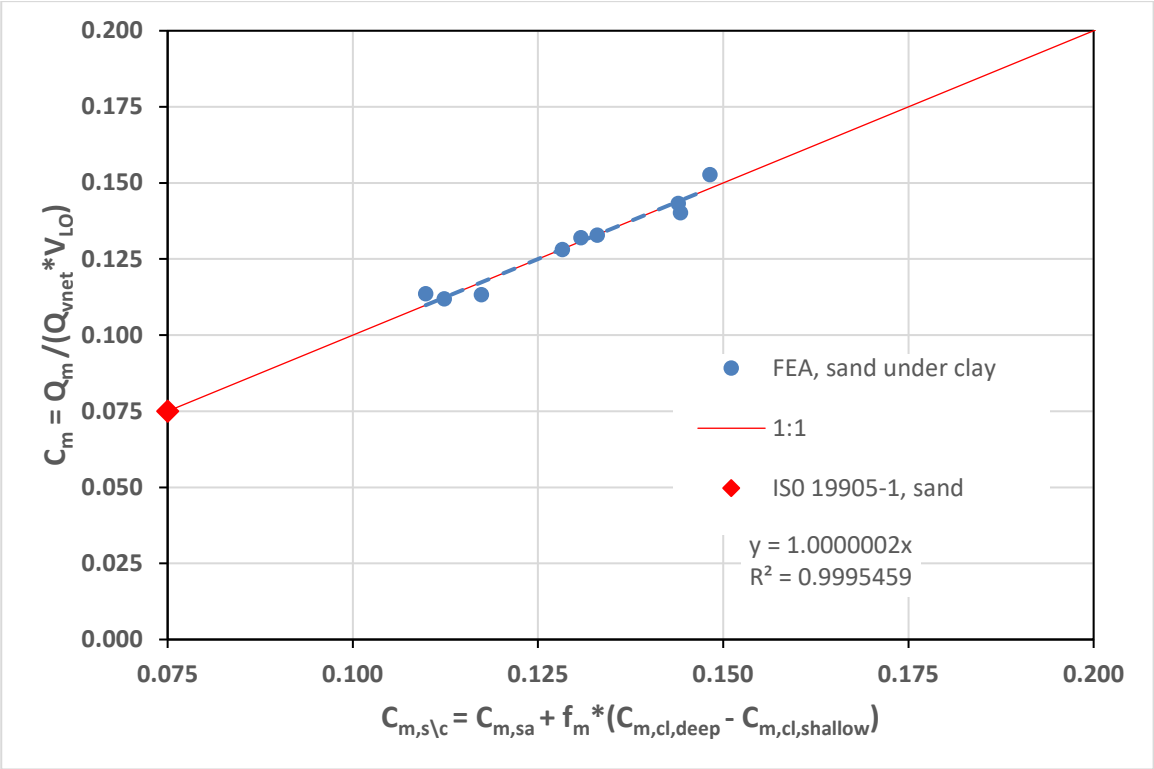

FIGURE 9: Plot of moment capacity factor, C_m, results vs. proposed correlation

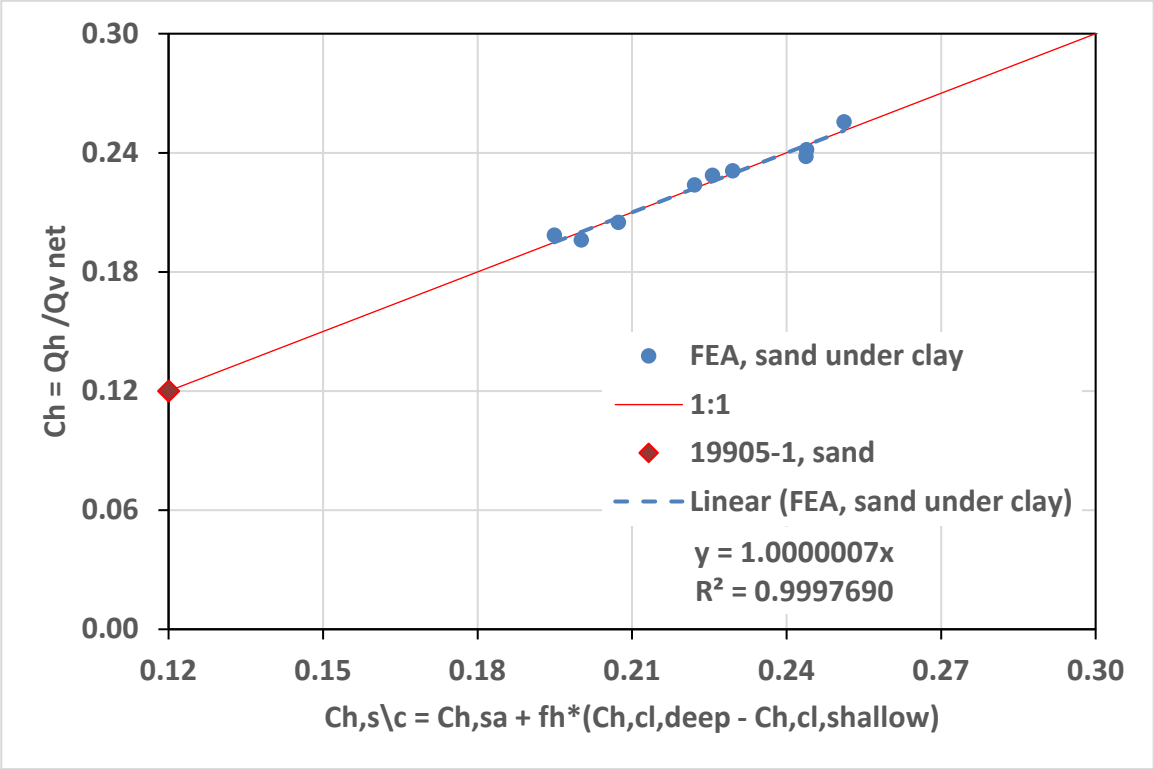

FIGURE 10: Plot of horizontal capacity factor, C_h, results vs. proposed correlation